Wireless Personal Communications (2024) 134:339–360
https://doi.org/10.1007/s11277-024-10911-z

RESEARCH

Comparative Analysis of End Device and Field Test Device Measurements for RSSI, SNR and SF Performance Parameters in an Indoor LoRaWAN Network

Ataberk Aksoy[1] · **Ömer Yıldız**[2] · **Sait Eser Karlık**[3]

Accepted: 10 February 2024 / Published online: 15 March 2024

Abstract
Internet of things phenomenon has brought up distinctive technologies that are using wireless communication and appearing in smart city applications. Long range (LoRa) modulation technique has pulled up the market and forced the announcement of LoRa wide area network (LoRaWAN) standard in 2021 by ITU-T with Y.4480 standard code. LoRaWAN is a medium access control protocol using low power wide area network approaches with the aim of long-range coverage and management of many end devices. LoRaWAN networks are emerging all over the world with some existing optimization, planning and network allocation problems that need to be overcome. This paper focuses on comparative analysis and interpretation of measurements performed in a LoRaWAN network deployed in an 18-floor building with a LoRaWAN gateway on the roof. The research covers results of comparative measurements between end device and Adeunis field test device (AFTD) for received signal strength indicator (RSSI), signal-to-noise ratio (SNR) and spreading factor (SF). End devices have been randomly selected from 18th, 12th, 6th and 1st floors and their daily performance data have been gathered through the network server. AFTD has been used to get 100 sample measurements for each floor. Maximum and average RSSI values obtained from end device measurements are higher than ones measured with AFTD except the case in the 18th floor. Excluding the maximum SNR values at the 1st and the 18th floors, all SNR values measured with AFTD are higher than ones obtained from end device measurements. SF measurements show that higher SF values are more likely to be used with increasing distances to the gateway as expected from the theoretical background.

✉ Ataberk Aksoy
502105013@ogr.uludag.edu.tr

Ömer Yıldız
511905009@ogr.uludag.edu.tr

Sait Eser Karlık
ekarlik@uludag.edu.tr

[1] MSc Program of Electronics Engineering, Graduate School of Natural and Applied Science, Bursa Uludağ University, Bursa, Türkiye

[2] PhD Program of Electronics Engineering, Graduate School of Natural and Applied Science, Bursa Uludağ University, Bursa, Türkiye

[3] Department of Electrical and Electronics Engineering, Faculty of Engineering, Bursa Uludağ University, Bursa, Türkiye

Keywords IoT · LoRa · LoRaWAN · Chirp spread spectrum · Smart city

1 Introduction and Related Works

1.1 Introduction

Internet of Things (IoT) was firstly announced in 1999 by Massachusetts Institute of Technology (MIT) Audible Lab. IoT technology is used to connect the Internet to the physical world through various sensors [1]. One of the fastest growing sectors in the IoT ecosystem is wireless communication technologies analyzed under two main titles as short and long range in terms of communication range [2]. The term 'low power consumption wireless area network (LPWAN)' defines some types of long-range wireless communication networks. There are different examples of LPWAN technologies such as long range (LoRa), Sigfox, narrow band-IoT (NB-IoT) [2]. LoRa is a long-range low power consuming wireless modulation technique derived from chirp spread spectrum (CSS) technology [3]. LoRa transmits small-size data (250 bytes) with low bit rates (200 kbps) within a range of 10–15 km in rural areas and 3–5 km in urban areas [4]. LoRa uses the frequency band range of 780–915 MHz in Europe and 902–928 MHz in United States [5]. LoRaWAN is a medium access control (MAC) layer protocol built over LoRa modulation [3]. The LoRaWAN protocol has been developed by the LoRa Alliance. The first LoRaWAN technical standard was published in January 2015 [3]. LoRaWAN end devices are optimized to operate in low power mode with a single button battery providing up to 10 years of operation [5]. LoRa gateways (GWs) have high sensitivity down to −137 dBm signal power level.

1.2 Related Works

LoRa applications are being discussed for different topics such as tracking devices [6], tracking objects [7], energy monitoring [8], urban vehicle localization [9], real time data gathering from vehicles in motion [10], car parking [11], air quality management [12], air quality monitoring through indoor applications like schools [13], water quality monitoring [14] and water management [15]. Furthermore, there are other applications related to agriculture which involves LoRaWAN-based wireless underground sensor to monitor below the level of soil [16] and error rate analysis using LoRa in health monitoring [17]. Additionally, another experimental research about smart parking service with LoRaWAN analyzes propagation models to understand the usability in city-scale networks as well as presenting some predictions based on artificial intelligence (AI) to enhance confidence in smart parking sensor readings [18].

On the other hand, LoRa network is also being analyzed for general transmission performance, the efficiency, the packet loss, the signal-to-noise ratio (SNR) and the received signal strength indicator (RSSI). One part of the performance analyses includes packet error rate results [19] while another discusses received packet numbers, RSSI and SNR values [20]. There are also LoRa simulations developed to analyze the packet loss, the energy consumption and the collision rate [21]. Besides, a simulation called LoRa-Multi Armed Bandit (LoRa-MAB) focuses on transmission rates [22]. Moreover, comparative LoRaWAN network analysis between physical and simulation results is also available [23]. On data delivery point of view, reliability with multiple gateways regarding LoRaWAN

networks has also been researched in [24], where a successful result with 35% improvement on packet delivery ratio has been demonstrated.

1.3 Contribution of This Research

In this research, measurement results of RSSI, spreading factor (SF) and SNR parameters in a LoRaWAN network have been analyzed and compared with results of same parameters obtained with a LoRaWAN certificated field test device. Measurements have been performed on an indoor LoRaWAN with a rooftop gateway (GW) that has been previously deployed in a building with 18 floors. 1-day long measurement results of RSSI, SF and SNR parameters from end devices of this indoor LoRaWAN network, which are located at 1st, 6th, 12th and 18th floors of the building, have been obtained. The obtained results have been compared with field test results provided from measurements performed at same floors with an Adeunis Field Test Device (AFTD), which is a LoRaWAN certificated field test device [25]. The contribution of this research can be stated as follows:

(i) LoRaWAN field tests mostly cover outdoor applications where research base designed hardware have been generally used [6, 11, 12]. In this research, field tests have been performed in a building with 18 floors where daily life continues and concrete obstacles are present in the environment. Therefore, the results of this research give clues in understanding indoor performance of LoRaWAN networks. Furthermore, a novel indoor data set has been originated with AFTD field test results in this research.

(ii) In the literature, the network performance measurements have been generally performed with end device measurements. Comparison of end device measurements with another field test device measurements have not been realized [14–17]. However, in this research, Adeunis field test device has been used to make field test measurements and compare them with LoRaWAN end device measurements for RSSI, SNR and SF parameters.

Section 2 gives detailed information about LoRa and LoRaWAN network architecture. The material and method used in the research is introduced in Sect. 3. Results and discussions are presented in Sect. 4.

2 LoRa and LoRaWAN

2.1 LoRa

LoRa is a CSS-based modulation technique. It transmits data using compressed high-intensity radiated pulse (CHIRP) waves. This method is similar to the method used by dolphins and bats to communicate. LoRa modulation is resistant to distortion and enables data transfer over long distances (5–15 km) with low power consumption. The term SNR is very important in wired and wireless communication. SNR is expressed in decibels (dB). SNR is expected to be greater than 0 dB to ensure successful communication [26]. However, LoRa modulation can successfully perform wireless communication down to − 20 dB SNR depending on the SF variable [27]. LoRa is a technique that allows user to send long-range signals and firstly used in military applications. While another main LPWAN technology is

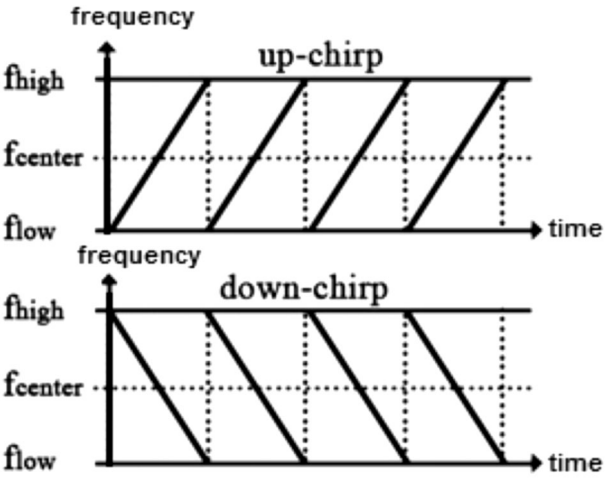

Fig. 1 Up-chirp and down-chirp signals

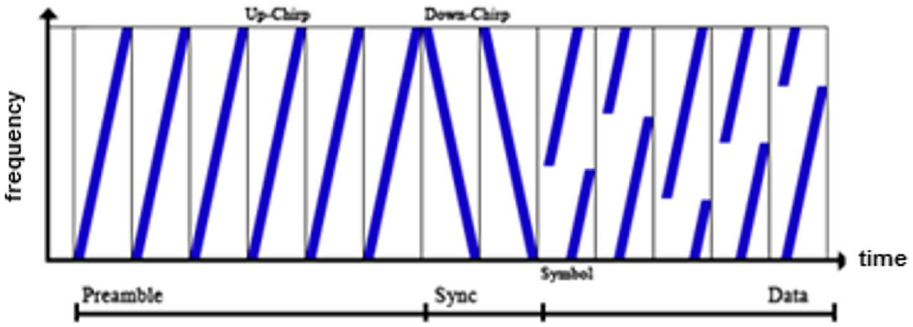

Fig. 2 CSS modulation

NB-IoT, there are differences in topics such as quality of service, battery life, network coverage, latency and cost between LoRa and NB-IoT [28]. There are various other LPWAN technology alternatives for LoRa namely as Sigfox, Dash7, Ingenu, Telensa, Weightless [29].

2.2 Chirp Spread Spectrum

CSS is a spread spectrum technique that uses broadband linear frequency modulated chirp pulses to encode data. It provides long-range performance with high reliability, strong resistance to interference and low power consumption. CSS has two types of signals, i.e., up-chirp and down-chirp [30].

Figure 1 shows the up-chirp and down-chirp signals that form the basis of CSS modulation [30].

The CSS modulation shown in Fig. 2 consists of three basic parts: preamble, synchronization and data [31]. The preamble section includes succession of up-chirps. The synchronization section following the preamble involves two down-chirps. If the receiver module receives two down-chirp signals after consecutive up-chirp signals, it understands that the message

encoded on chirp signals has arrived [31]. A chirp signal consists of $M=2^{SF}$ chips. A chirp signal can encode as many bits as SF number [31].

Chirp signal includes a short-time frequency expansion based on four parameters: *SF*, maximum frequency (f_{max}), minimum frequency (f_{min}) and input bits. The period of chirp signal, i.e., T_s, can be computed with [32]

$$T_s = \frac{M}{f_{max} - f_{min}} = \frac{2^{SF}}{f_{max} - f_{min}} \tag{1}$$

where $f_{max} - f_{min}$ shows the bandwidth.

Variation of the instant frequency (Δf) with time in a chirp signal is shown in Fig. 3. According to Fig. 3, the chirp signal has bandwidth (B), SF, symbol value (s) and the instant in time axis at which Δf wraps around (T_h). In LoRa modulation, the bandwidths are 125 kHz, 250 kHz and 500 kHz, SF differs between 7 and 12, s changes from 0 to M-1 chips. For the case in Fig. 3, the bandwidth is 500 kHz, SF is 8 and s is the 91th chip. Using (1) and values given above, the chirp signal period T_s can be computed as 5.12×10^{-4} s. $\Delta f(s,t)$ has a starting value of $\frac{-B}{2} + \frac{B}{M}.s$ Hz and increases linearly. When $\Delta f(s,t)$ reaches to the value of $\frac{B}{2}$ Hz, it wraps around to the value of $-\frac{B}{2}$ Hz at the T_h value of the time axis and increases linearly again till the starting value of $\Delta f(s,t)$. The starting value of $\Delta f(s,t)$ can be computed as -0.723×10^5 Hz for the case in Fig. 3. The value of T_h can be computed with [32]

$$T_h = T_s - \frac{T_s}{M}.s \tag{2}$$

Using (2), the value of T_h can be calculated as 3.3×10^{-4} s for the case in Fig. 3.

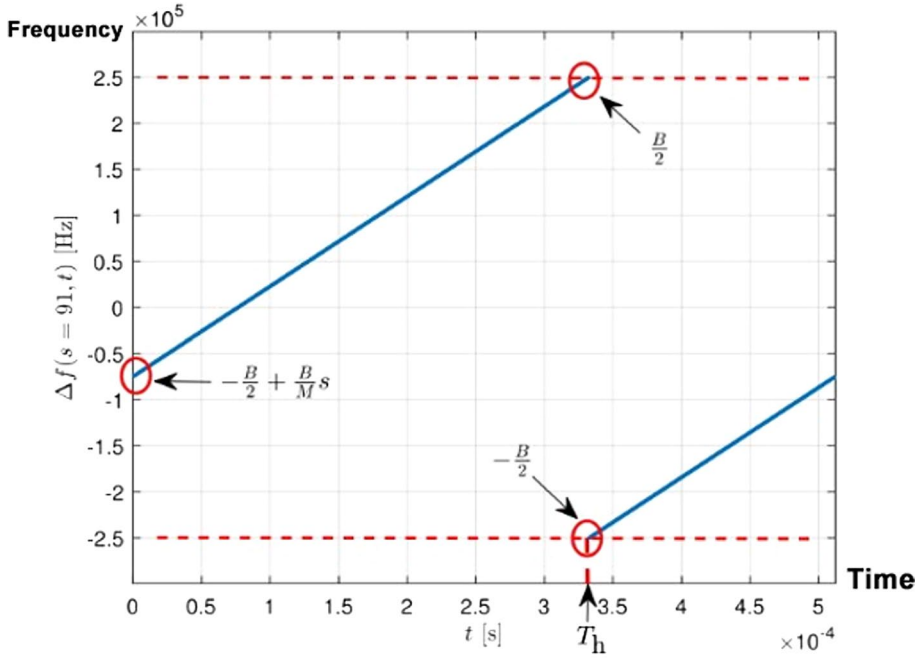

Fig. 3 Variation of the instant frequency with time in a chirp signal

Figure 4 presents time–frequency relation for SF values varying from 7 to 12 and bandwidths of 125 kHz, 250 kHz and 500 kHz used in LoRa modulation [33].

2.3 Spreading Factor

LoRa modulation uses six different SF values from SF7 to SF12. SF controls the speed of data transmission by controlling the chirp rate. If the RSSI is lower than the noise floor, it is not normally possible to demodulate the signal. However, LoRa can demodulate signals below the noise floor thanks to the SF variable [34].

Figure 5 shows the variation of a chirp signal from left to right from SF7 to SF12. In a communication system, increasing the bandwidth increases the bit rate. However, using a wider bandwidth causes the system to consume much more power. SF changes the length of the signal on the time axis while keeping the bandwidth constant. Increasing the SF value causes the bit rate of the transmitted signal to decrease. However, higher SF values are more resistant to distortion. Therefore, high SF values can be used for long-range communication. Table 1 gives the relation between SF and RSSI limit, i.e. the receiver sensitivity, for 125 kHz bandwidth [34]. The lower the RSSI value, the lower the signal strength. The signal strength is lower in noisy environments. As it is obvious in Table 1, increasing the SF variable allows the RSSI limit to decrease to lower values. Higher SF values are therefore used when operating in noisier environments.

Table 2 shows the changes in various parameters depending on SF values for 125 kHz bandwidth [35]. As shown in Table 2, increasing the SF value increases the number of chips used. In this way, larger size data can be sent. As the SF value increases, the signal will become more resistant to distortion. In this way, it will be possible to communicate

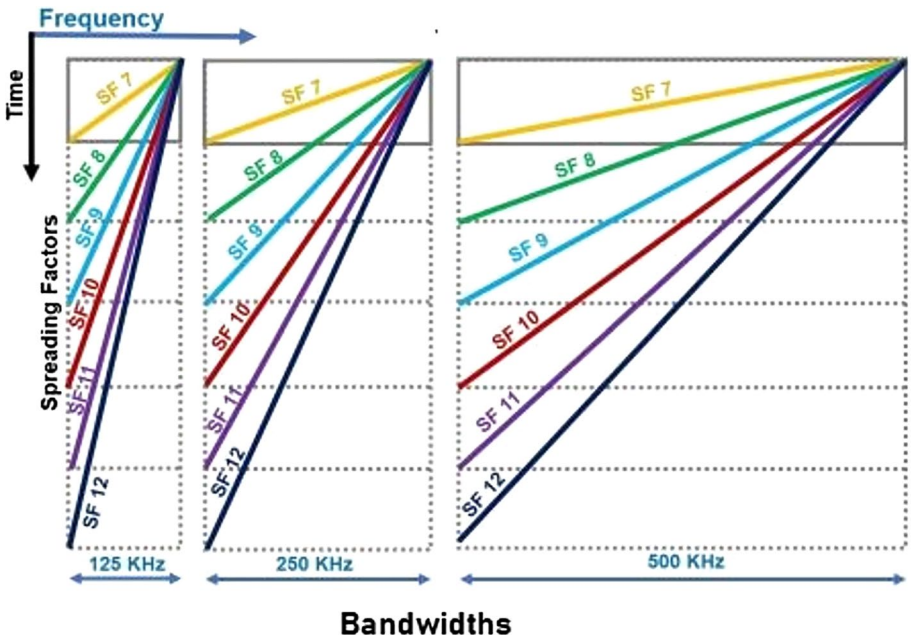

Fig. 4 Time versus frequency variation for different SF and bandwidth values

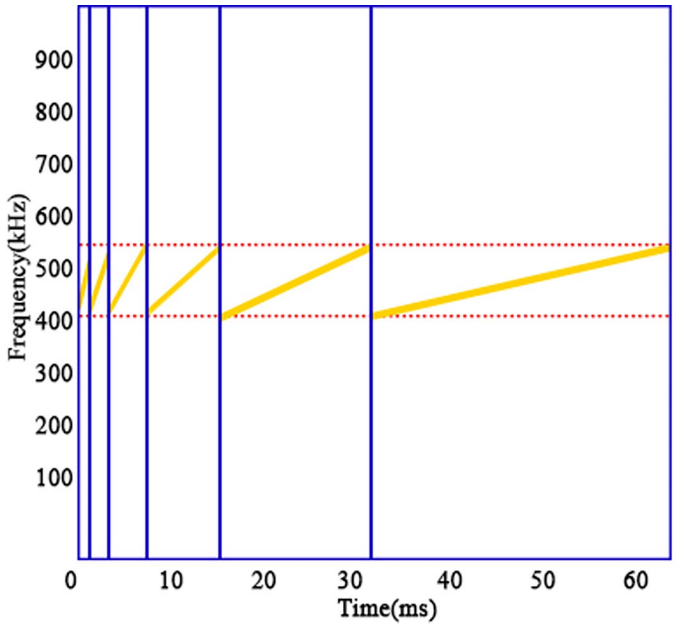

Fig. 5 Spreading factor values

Table 1 The matching table of SF values to RSSI values giving the receiver sensitivity

SF value	RSSI limit (dBm)
SF7	– 123
SF8	– 126
SF9	– 129
SF10	– 132
SF11	– 134.5
SF12	– 137

Table 2 The matching table of SF values to number of chips, SNR limits, time-on-air (ToA) durations and bit rates

SF value	Chips	SNR limit (dB)	ToA (for 10-byte packet) (ms)	Bit rate (bps)
SF7	128	– 7.5	56	5469
SF8	256	– 10.0	103	3125
SF9	512	– 12.5	205	1758
SF10	1024	– 15.0	371	977
SF11	2048	– 17.5	741	537
SF12	4096	– 20.0	1483	293

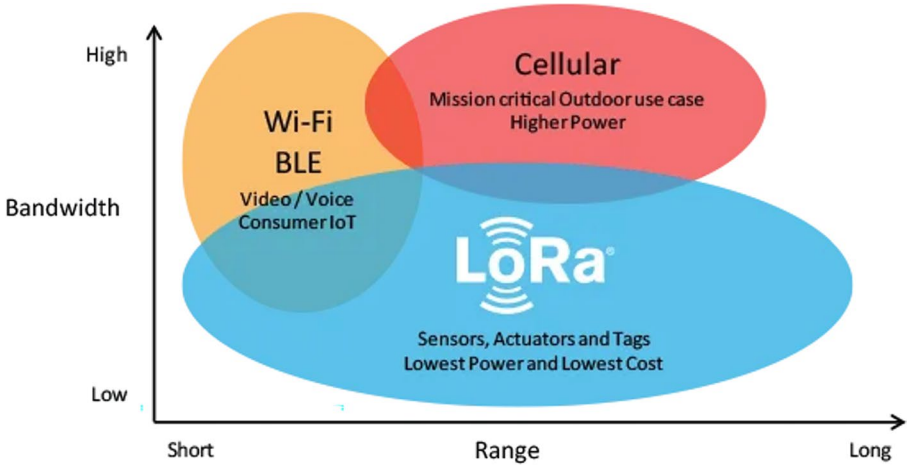

Fig. 6 LoRa and other wireless communication technologies

Table 3 Regional LoRaWAN frequencies

Region	Frequency band (MHz)
China	779–787
EU	863–870 and 433
US	902–928

successfully at lower SNR values. Increasing the SF value will decrease the bit rate, so the data packet will be transmitted in a longer time.

To be more precise and to evaluate the contents of Tables 1 and 2 together, it can be said that three key parameters of LoRa-based systems are SF, SNR and RSSI. Tables 1 and 2 show the limits and thresholds for the relations SF-RSSI and SF-SNR. Since $SNR < 0$ means that the signal power is lower than noise power or in other words the signal is under the noise floor, the LoRa-based systems ensure that the signal can be received with negative SNR as shown in Table 2. Because of negative SNR, in noisy environments, the receiver sensitivity should reach much lower values to be able to detect the signal under the noise floor. Table 1 shows that this can be handled by increasing the SF values from 7 to 12 in LoRa-based systems to reach much lower RSSI values, i.e. receiver sensitivities.

2.4 LoRaWAN

LoRaWAN is suitable for transmitting small size data such as sensor data over long distances since LoRa modulation provides longer range communication with lower bandwidths than other wireless communication technologies [3]. Figure 6 shows some of the access technologies that can be used for wireless communication and their bandwidths vs. the expected communication range [3].

Table 3 shows the regional operating frequencies of LoRaWAN [36].

Figure 7 shows the LoRaWAN network architecture [36]. LoRaWAN network consists of four basic parts: end devices, gateway (GW), network server and application server. End

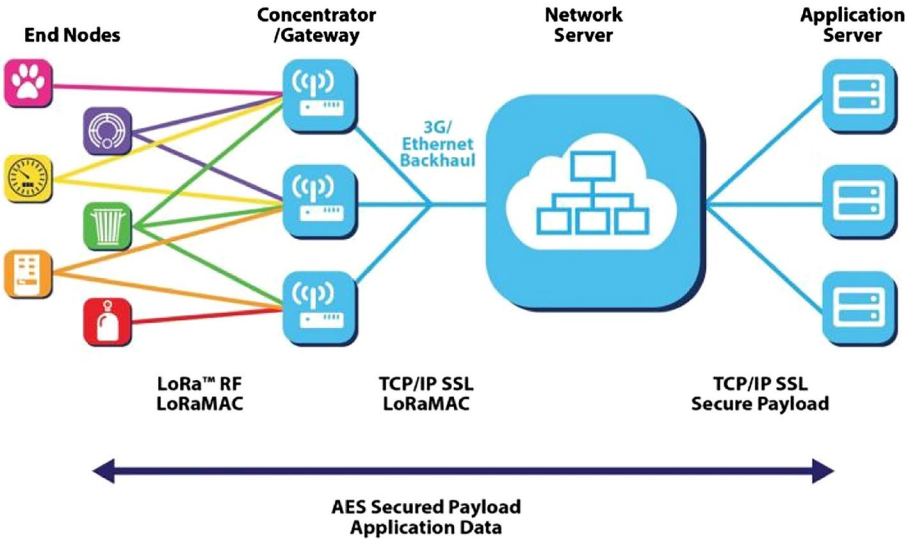

Fig. 7 LoRaWAN network architecture

devices are connected to the gateway with a star topology network structure. Due to the star topology, sensors cannot communicate directly with each other, they exchange data through the gateway. The communication between the end devices and the gateway is bidirectional. Sending data from the end device to the gateway is called "uplink" and sending data from the gateway to the end device is called "downlink". Gateways are the key devices that enable connectivity in IoT. Gateways are responsible for converting the data sent by end devices in the form of radio frequency (RF) packets into Internet protocol (IP) packets. The gateways transfer the converted IP packets to the cloud. The network server is in charge of managing gateways, end devices, applications and users across the entire LoRaWAN network. The network server verifies the authenticity of end devices and the integrity of messages. It responds to all MAC layer commands. The application server is tasked with processing application-specific data messages received from end devices. There can be more than one application server in a LoRaWAN [37]. There are three basic LoRaWAN classes; A, B, C. Class A devices are battery powered and have the lowest power consumption. They spend most of their time in sleep mode. Class A devices have bidirectional communication. Class A devices can only communicate with one gateway. Class A devices are generally used in areas such as environmental and location monitoring [38], radon risk management [39], forest fire detection [40], earthquake monitoring [41], animal tracking [42], water supply monitoring [43], water monitoring and leakage detection in housing complexes [44]. Class B devices have shorter battery life than Class A devices because they spend more time during beacons and ping slots while in active mode. Bidirectional communication is possible with receive slots. Class B devices can communicate with multiple gateways at the same time. Class B devices are generally used in areas such as auxiliary counters and temperature reporting [38]. Class C devices are the most power consuming class among all devices. They are usually connected to the electrical network. Class C devices have bidirectional communication. Class C devices can communicate with multiple gateways at the same time. Class C devices are generally used in areas such as switched utility meters and streetlights [26].

The LoRaWAN uplink and downlink frame formats are given in Fig. 8 [45]. The uplink frames are transmitted from end devices to the GW while downlink frames generated by LoRaWAN network server are sent to end devices from the GW.

The preamble of LoRaWAN frames shown in Fig. 8 helps in synchronizing the receiver and the transmitter. It contains 8 symbols. The physical header (PHDR) contains information about sizes of the payload and the cyclic redundancy check (CRC). The physical header CRC (PHDR-CRC) involves an error detection code used to detect errors in the header. The PHYPayload includes the whole frame that is generated by the MAC layer. The maximum size of the payload, which is region-specific, varies with the data rate. CRC contains an error detection code used to detect errors in the payload of uplink messages [45].

3 Material and Method

Measurements have been performed on the 18th, 12th, 6th and 1st floors of an 18-floor building with a LoRaWAN gateway (GW) on its roof, as shown in Fig. 9. Class A end devices, which are LoRaWAN certified water-meters, are used on floors in the LoRaWAN under test. The end devices are placed in the elevator shaft of the building as shown in Fig. 10. They are located at vertically proportional distances to the GW at the roof. The structural properties of the building, e.g., the thickness of the concrete, densities of steel and wood, are similar in all floors. One-day measurement results of the performance parameters, i.e., RSSI, SNR and SF values, obtained from end devices located at the floors stated above have been compared with measurements obtained from same floors with AFTD. The number of measurements performed with AFTD at each floor is 100.

The schematic representation of a floor where the LoRaWAN end device is installed and the measurements have been performed with AFTD is given in Fig. 11. Point 1 in the elevator shaft represents the location of the LoRaWAN end device, i.e. the water-meter, point 2 represents the location where the measurements have been made with AFTD. The distances between end devices on the 18th, 12th, 6th and 1st floors and the gateway on the roof are 7.07 m, 23.5 m, 41.3 m and 56.2 m, respectively.

Each floor has a total closed area of 900 m^2 and involves 4 apartments. The plans of all floors are the same. Since the apartments are not empty, the measurements have been performed at points closest to end devices with a maximum distance of 1 m and located outside the apartments due to inviolability of domicile issues. Construction materials at the floor around the measurement area are concrete, wooden doors and the elevator shaft.

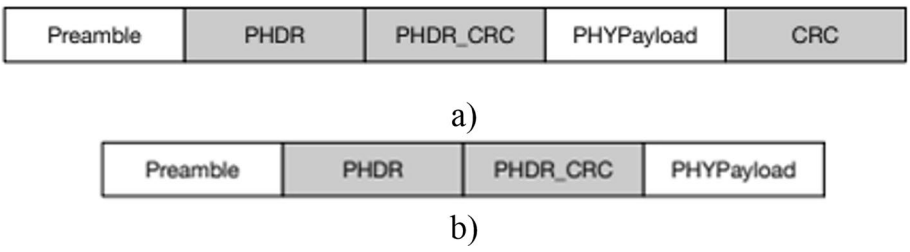

Fig. 8 LoRaWAN **a**) uplink and **b**) downlink frame formats

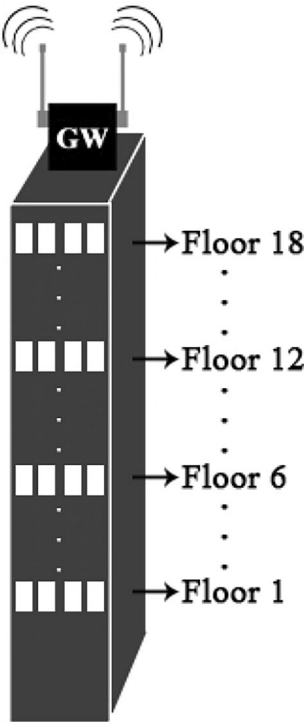

Fig. 9 The schematic representation of the building where the LoRaWAN under test is installed

Fig. 10 The end-device (water-meter) installed in the elevator shaft of the building

RSSI, which has a negative value, is measured in dBms and represents the power of the received RF signal. As the RSSI value approaches to zero, stronger signals are received. RSSI can increase or decrease depending on environmental factors, fading, attenuation etc. SF value can get values between 7 and 12. SNR is the ratio of the received RF signal power to the noise power. On behalf of LoRaWAN equipment, GW communicates with end devices and forward messages between end devices and the network server. The network

Fig. 11 The schematic representation of a floor where the LoRaWAN end device is installed

server keeps RSSI, SNR and SF information measured during communication. Throughout the research, the performance data of end devices located at 1st, 6th, 12th and 18th floors have been analyzed focusing on RSSI, SNR and SF parameters. The data packets transmitted with LoRa-CSS modulation contain consumption data of the water-meters and details of data packets are inaccessible due to security reasons. The network is active. The structure of a single frame is the same as the LoRaWAN frame structure given in Fig. 8. The measurements have not been performed within a single floor. Firstly, measurements have been made on the 18th floor, which is the closest floor to the gateway, and then on the 12th, 6th and 1st floors, respectively. In measurements, the uplink packets transmitted successfully from the end device in each floor to the gateway have been considered. The gateway used during the research satisfies LoRaWAN standards with radio signal transmission features shown in Table 4.

Non-line-of-sight (NLOS) conditions are present for radio signal transmission between end-devices and the gateway for the test environment. Topics like multipath propagation, signal fading, etc. have not been concentrated on in this research but they will be focused on in subsequent future ones.

The network performance has been observed and evaluations have been given with respect to SNR, RSSI and SF parameters. The measurement data has been transferred to the desktop computer via the IoT configurator application of the AFTD and it has been processed in Excel files in the digital environment to create the relevant tables and graphs. Excluding Adeunis IoT configurator, no other simulation software, third party libraries or open source software have been used in this research. The field tests with AFTD have been

Table 4 Radio signal transmission features for the gateway

Feature	Value
Antenna gain	4.5 dBi
Antenna type	Omnidirectional
Tx power	14 dBm
Frequency band	868 MHz

performed as 4 different floor tests, i.e. floor 18, floor 12, floor 6 and floor 1 tests, with the same method used in end device measurements.

4 Comparative Measurement Results and Performance Analysis

Table 5 shows the comparative RSSI results obtained from one-day measurements of the end devices and from 100 sample AFTD measurements performed at the same floors in different days due to test environment and network data access restrictions. The duration of a single test with AFTD has lasted about 2 minutes in the test area. Therefore, the total test duration for one floor has taken about 200 minutes and total test duration in the building has been about 800 minutes.

The RSSI measurement results show that both AFTD and end devices have acceptable average, maximum and minimum values compared to the values given in [12]. When the average RSSI values are analyzed, the end device measurement results show approximately an 8 dB variation between −98.92 dBm and −107 dBm. The variation in average RSSI values obtained from AFTD results is approximately 30 dB between −89.34 dBm and −119.78 dBm. When the maximum RSSI values are analyzed, the measurement results for the end devices show a variation of 13 dB between −92 dBm and −105 dBm, while the maximum AFTD results show a variation of 30 dB between −85 dBm and −115 dBm. Finally, when the minimum RSSI values are analyzed, the AFTD results show a variation of 27 dB between −97 dBm and −124 dBm, while the end device results show a variation of 7 dB from −109 dBm to −116 dBm. When all variations in all RSSI results are analyzed, the average RSSI variation in the end device results is 9.36 dB, while the average RSSI variation in the AFTD results is 29.15 dB. As shown in Table 5, the highest and the lowest RSSI values are both observed in AFTD measurements with −85 dBm at the 18th floor and with −124 dBm at the 1st floor, respectively.

The boxplot representation of distribution of RSSI values obtained from measurements of LoRaWAN end devices and AFTD measurements are given in Figs. 12 and 13, respectively. When the maximum and average RSSI values are analyzed, it is obvious that RSSI values increase with the increase in floor numbers from the 1st to the 18th floor in both Figs. 12 and 13. But when the minimum RSSI values are analyzed, it is seen that the minimum RSSI values in Fig. 12 decrease between the 6th and the 12th floor contrary to the general expectations while the minimum RSSI values in Fig. 13 increase with increasing

Table 5 Comparative RSSI results obtained from end devices and AFTD measurements

Floor	LoRaWAN end device results			AFTD results		
	Average RSSI (dBm)	Maximum RSSI (dBm)	Minimum RSSI (dBm)	Average RSSI (dBm)	Maximum RSSI (dBm)	Minimum RSSI (dBm)
18	−98.92	−92	−109	−89.34	−85	−97
12	−105	−95	−115	−107.98	−102	−113
6	−106.60	−102	−114	−110.63	−107	−115
1	−107	−105	−116	−119.78	−115	−124

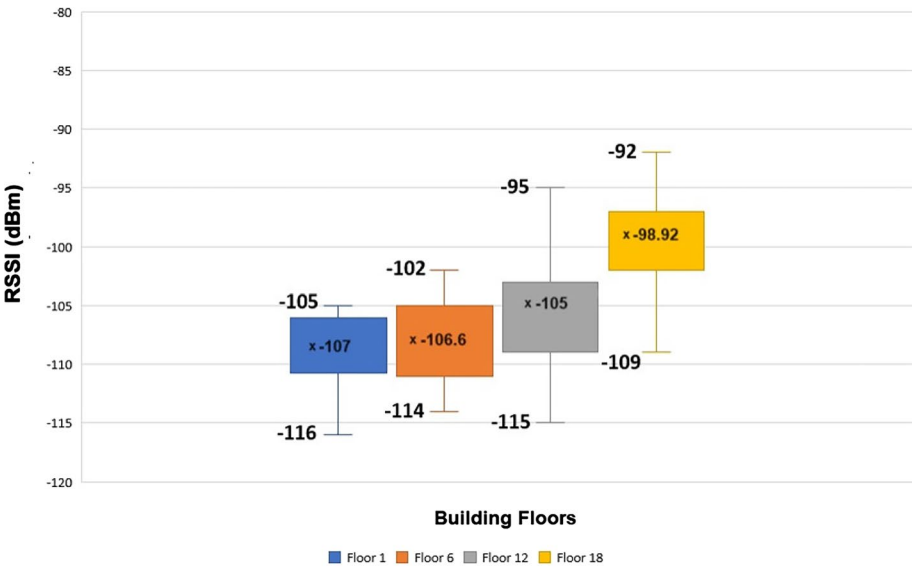

Fig. 12 The boxplot representation of distribution of RSSI values obtained from LoRaWAN end devices

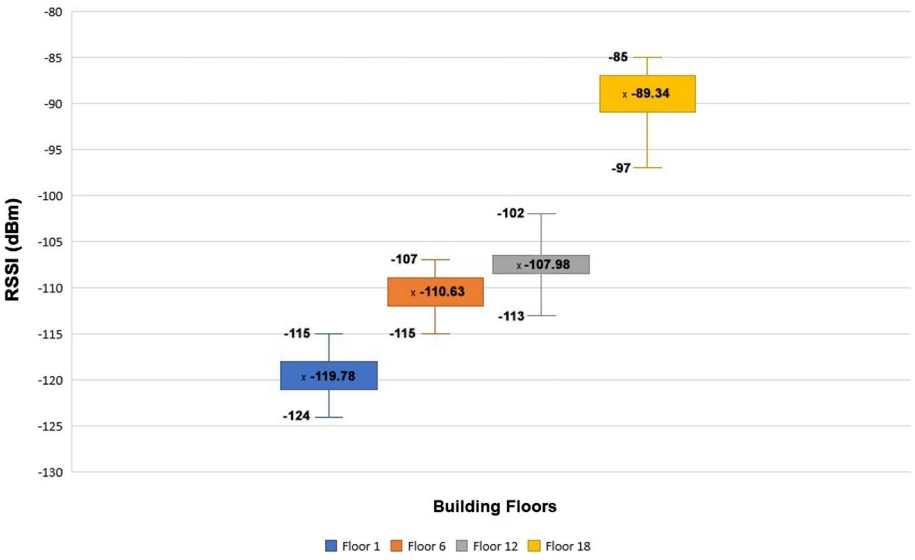

Fig. 13 The boxplot representation of distribution of RSSI values obtained from AFTD measurements

floor numbers. This shows that the instantaneous RSSI values can vary depending on not only the distance to GW but also environmental factors.

Table 6 shows the comparative SNR values obtained from measurements of end devices and from measurements with AFTD. In line with expectations, the average SNR values decrease with increasing distance to the GW for both end device measurements and AFTD

Table 6 Comparative SNR results obtained from end devices and AFTD measurements

Floor	LoRaWAN end device results			AFTD results		
	Average SNR (dB)	Maximum SNR (dB)	Minimum SNR (dB)	Average SNR (dB)	Maximum SNR (dB)	Minimum SNR (dB)
18	3.99	8.5	−5.2	6.4	8	4
12	0.18	5.5	−9.8	3	6	−2
6	−5.93	2.5	−13.8	2.4	4	−1
1	−6.1	1	−13.2	−4.9	−4	−8

measurements as shown in Table 6. SNR measurements emphasize that LoRaWAN can also operate at negative SNR values. The average SNR obtained from end device measurements decreases from 3.99 to −6.1 dB between the 18th and 1st floors. Similarly, the average SNR obtained from AFTD measurements decreases from 6.4 to −4.9 dB between the 18th and 1st floors. The maximum SNR obtained from end device measurements decreases from 8.5 dB to 1 dB between the 18th and 1st floors while similarly, the maximum SNR obtained from AFTD measurements decreases from 8 to −4 dB. The minimum SNR obtained from end device measurements decreases from −5.2 to −13.2 dB between the 18th and 1st floors while similarly, the minimum SNR obtained from AFTD measurements decreases from 4 to −8 dB.

The boxplot representation of distribution of SNR values obtained from measurements of LoRaWAN end devices and AFTD measurements are given in Figs. 14 and 15, respectively. The average SNR variation between the first and the last floors for the end device measurements is 10.09 dB in Fig. 14 while it is 11.3 dB for AFTD measurements in Fig. 15. As shown in Figs. 14 and 15, average and maximum SNR values increase with decreasing distance to the GW from the 1st to the 18th floors in both end device measurements

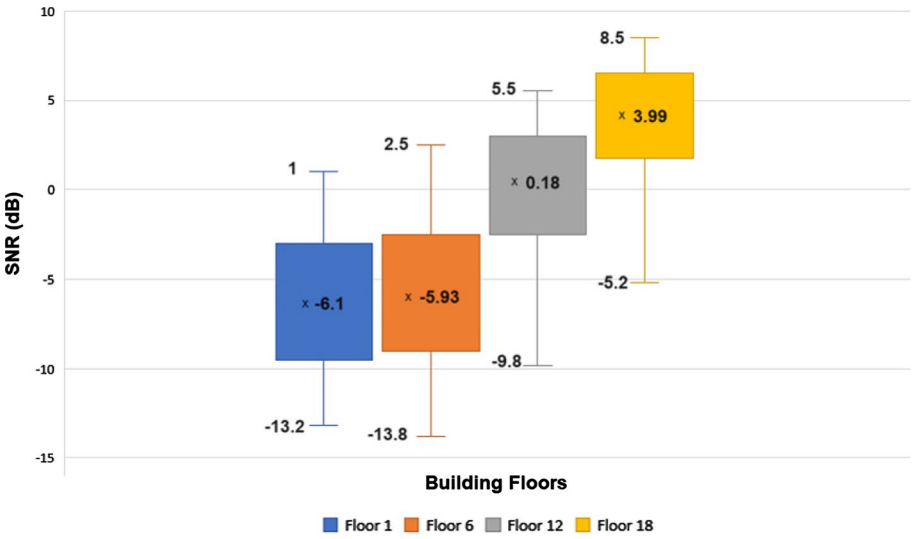

Fig. 14 The boxplot representation of distribution of SNR values obtained from LoRaWAN end devices

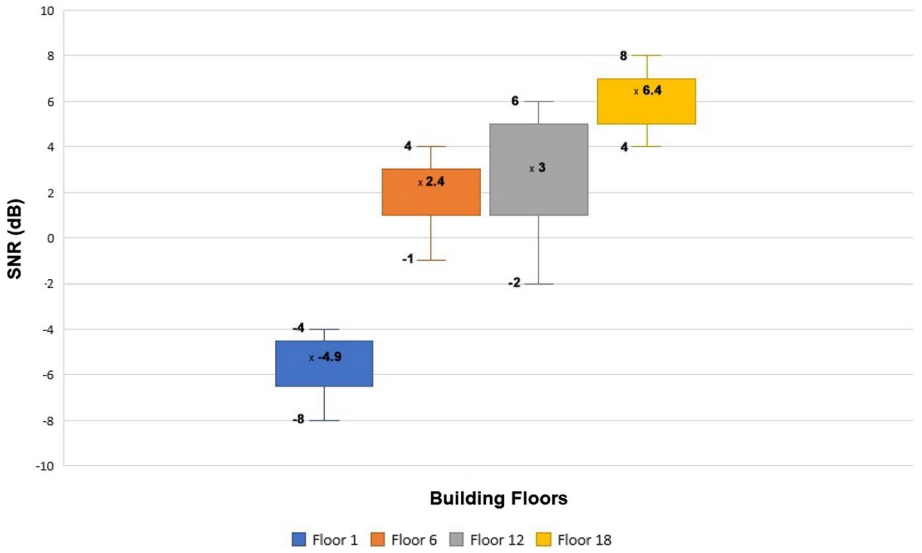

Fig. 15 The boxplot representation of distribution of SNR values obtained from AFTD measurements

and AFTD measurements parallel to the general expectations. The same pattern occurs for minimum SNR values but with exceptions at the 6th floor for end device measurements in Fig. 14 and at the 12th floor for AFTD measurements in Fig. 15. These can be attributed to the environmental factors similar to the case occurred in RSSI measurements.

In Table 7, comparative allocation numbers of SF values in all measurements performed by using both the end device and AFTD for each floor under test are given. Since SF values are assigned automatically in the LoRa protocol, the numbers shown in Table 7 emphasize how many times SF 7–12 values have been allocated automatically at the floors during the measurements. From a different point of view, values given in Table 7 show numbers of successful links formed between the end device/AFTD and the LoRaWAN network during measurements, e.g. at the 18th floor, the end device use 38 SF7 value and 1 SF12 value in establishing a total of 39 successful links in the test day. While moving from 18th floor to the 1st floor, the numbers of successful link establishments decrease and the numbers of allocated SF values change with increasing distance to the GW for end devices. Almost all successful link establishments are achieved with

Table 7 Comparative allocation numbers of SF values in all measurements

Floor	In LoRaWAN end device measurements allocation numbers of						In AFTD measurements allocation numbers of					
	SF 7	SF 8	SF 9	SF 10	SF 11	SF 12	SF 7	SF 8	SF 9	SF 10	SF 11	SF 12
18	38	–	–	–	–	1	100	–	–	–	–	–
12	18	12	–	–	1	4	34	42	16	8	–	–
6	–	8	–	1	13	1	–	9	16	23	32	20
1	–	–	6	8	–	4	–	–	–	–	3	97

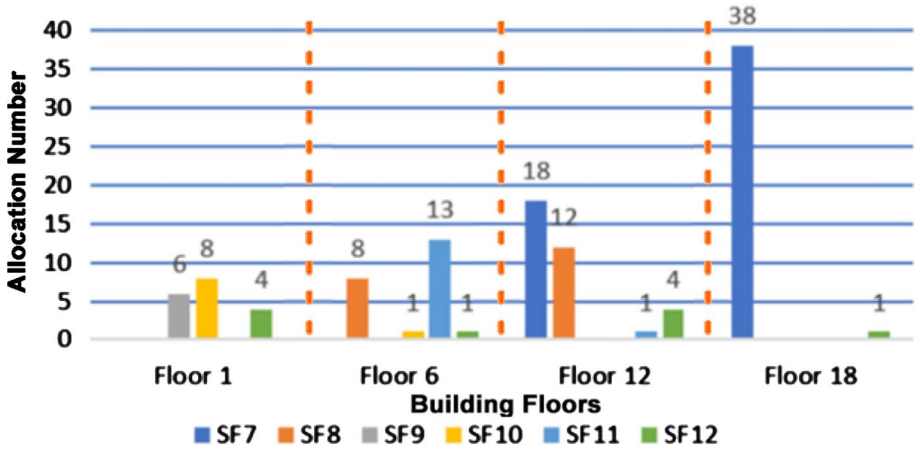

Fig. 16 The bar diagram of allocation numbers of SF values for end devices

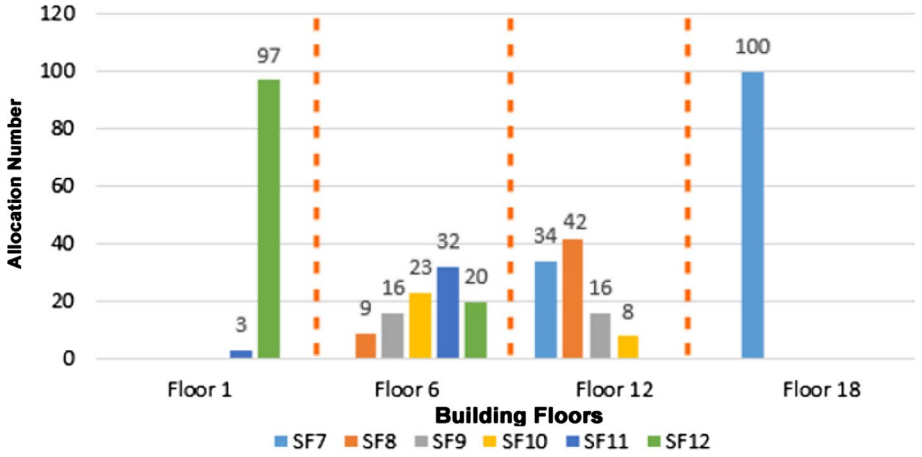

Fig. 17 The bar diagram of allocation numbers of SF values for AFTD device

SF7 in the 18th floor in end device measurements similar to the case for AFTD measurements performed in the same floor. Looking at the 12th floor, end devices communicate with SF11 and SF12 as well as SF7 and SF8 however AFTD communicates with SF9 and SF10 as well as SF7 and SF8. On the 6th floor, more than 50% of the total communications is achieved with SF11 while SF8, SF10 and SF12 are also used in end device measurements. However, for AFTD measurements at the same floor, 32% of the total communications is achieved with SF11 while SF8, S9, SF10 and SF12 are also used. For the 1st floor, SF values used in end device measurements and AFTD measurements are somewhat different. AFTD operates with mainly SF12 and also SF11 while end devices operate with SF9, SF10 and SF12 at the first floor.

The bar diagram of allocation numbers of SF values for end devices at floors under test is given in Fig. 16 while a similar bar diagram is shown in Fig. 17 for AFTD device.

It is obvious in both Figs. 16 and 17 that smaller SF values are more likely used as the distance to the GW decreases. Furthermore, with decreasing distance to GW at higher floors, the number of successful connections increases in Fig. 16.

5 Conclusion

In this paper, 1-day long measurement results of RSSI, SNR and SF values obtained from end devices of a LoRaWAN network located at 18th, 12th, 6th and 1st floors of an 18-floor building have been compared with results obtained from AFTD field tests performed at the same floors. For each floor, 100 AFTD field measurements have been made. The total AFTD test duration in the building has lasted about 800 minutes. Due to test environment and network data access restrictions, AFTD field tests have been performed in different days. Therefore, physical factors such as variations in ambient conditions, human density, and network traffic density can be the reason for the differences of the RSSI, SNR and SF values obtained from end devices with respect to the values measured with AFTD.

Considering results of RSSI measurements in Table 5, LoRaWAN end device results are higher than AFTD results, excluding results in 18th floor, for average and maximum RSSI values. For minimum RSSI results, AFTD results have lower values in 12th and 18th floors and higher values in 1st and 6th floors with respect to end devices. The variation of average RSSI values between the first and last floors of the building where the LoRaWAN is implemented is approximately 30 dB for AFTD measurements and 8 dB for end device measurements.

According to SNR measurement results, average SNR margin has been found to be 10 dB for end device measurements and 11.3 dB for AFTD measurements. Comparative allocation numbers of SF values in all measurements show that end device behavior and AFTD behavior in SF value allocation are different from each other.

The measurement results presented in this paper show that LoRa end devices can successfully perform wireless communication under negative SNR values, whose minimum value has been detected as -13.8 dB in the LoRaWAN under test.

In this research we have used a LoRaWAN network that has been already deployed. Therefore, we have had no chance to analyze topics such as transmitted and received uplink packets and the packet loss since they have not been accessible for this network. However we have plans to establish another LoRaWAN network, instead of using an already established one where we have to deal with such restrictions, and to perform additional analysis including those topics in our future works.

In future works, in addition to the end device and AFTD measurements, computer simulations focusing on impacts of environmental conditions on the LoRaWAN system performance are also being planned to study on. Furthermore, optimization in LoRaWAN network based on casual analysis of network performance is another topic for our future research interests. We believe that real network and AFTD result comparison method will give chance to create a novel optimization method for this kind of LoRaWAN networks that have been already established. Before and after optimization results will be also meaningful and competitive solution assistant for huge LoRaWAN networks. Moreover, focusing on multipath propagation and signal fading issues as well as environmental condition analysis in future research will also be helpful to gain an in-depth understanding of such indoor LoRaWAN network performances.

Acknowledgements This research was achieved with the permission of BUSKI (Bursa Metropolitan Municipality Water and Wastewater Management Authority) given in 2021.

Authors' Contributions AA: Conceptualization, Methodology, Formal Analysis, Investigation, Resources, Data Curation, Visualization, Writing-Original Draft. ÖY: Conceptualization, Methodology, Formal Analysis, Investigation, Resources, Data Curation, Visualization, Writing-Original Draft. SEK: Conceptualization, Methodology, Investigation, Resources, Data Curation, Visualization, Writing-Review and Editing, Supervision, Project Administration.

Funding The authors declare that no funds, grants, or other support were received during the preparation of this manuscript.

Data Availability The datasets generated and/or analyzed during the current study are available from the corresponding author on reasonable request.

Code Availability Not applicable for this manuscript.

Declarations

Conflict of interest The authors have no relevant financial or non-financial interests to disclose.

References

1. MIT Auto-ID Laboratory. (2023). https://autoid.mit.edu/
2. Liya, L., & Aswathy, M. (2020). LoRa technology for Internet of Things (IoT): A brief survey. In *2020 Fourth international conference on I-SMAC (IoT in Social, Mobile,* M. *Analytics and Cloud) (I-SMAC'2020)* (pp. 8–13). https://doi.org/10.1109/I-SMAC49090.2020.9243449
3. What are LoRa and LoRaWAN? (2022). https://www.thethingsnetwork.org/docs/lorawan/what-is-lorawan/
4. Sundaram, J. P. S., Du, W., & Zhao, Z. (2020). A survey on LoRa networking: Research problems, current solutions and open issues. *IEEE Communications Surveys and Tutorials, 22*(1), 371–388. https://doi.org/10.1109/COMST.2019.2949598
5. Tardy, I. C. R., Aakvaag, N., Myhre, B., & Bahr, R. (2017). Comparison of wireless techniques applied to environmental sensor monitoring. *SINTEF Report*, A27942, pp. 15–16. https://sintef.brage.unit.no/sintef-xmlui/handle/11250/2436270
6. de Camargo, E. T., Spanhol, F. A., & e Souza, A. R. C. (2021). Deployment of a LoRaWAN network and evaluation of tracking devices in the context of smart cities. *Journal of Internet Services and Applications, 12*, 8. https://doi.org/10.1186/s13174-021-00138-7
7. Kim, D. Y., Park, J. B., Shin, J. H., & Kim, J. D. (2017). Design and implementation of object tracking system based on LoRa. In *2017 International conference on information networking (ICOIN'2017)* (pp. 463–467). https://doi.org/10.1109/ICOIN.2017.7899535
8. Zhou, B. (2021). Energy-efficient, environment-aware synchronization and connectivity for the Internet of Things. Ph.D. dissertation, University of Nebraska, Lincoln, Nebraska. https://www.proquest.com/dissertations-theses/energy-efficient-environment-aware/docview/2529979887/se-2
9. Li, Y., Barthelemy, J., Sun, S., Perez, P., & Moran, B. (2022). Urban vehicle localization in public LoRaWan network. *IEEE Internet of Things Journal, 9*(12), 10283–10294. https://doi.org/10.1109/JIOT.2021.3121778
10. Di Renzone, G., Parrino, S., Peruzzi, G., & Pozzebon, A. (2021). LoRaWAN in motion: Preliminary tests for real time low power data gathering from vehicles. In *2021 IEEE international workshop on metrology for automotive (MetroAutomotive'2021)* (pp. 232–236). https://doi.org/10.1109/MetroAutomotive50197.2021.9502882
11. Zhuang, Y. (2019). Wireless parking detection system based on sensor fusion and IoT communication. M.Sc. Thesis, University of Washington. https://www.proquest.com/dissertations-theses/wireless-parking-detection-system-based-on-sensor/docview/2305852659/se-2
12. Kantilal, B. V. (2021). IoT based air quality monitoring system with power consumption optimization and air quality parameters prediction using deep learning. Ph.D. dissertation, The Maharaja Sayajirad University of Baroda. https://www.proquest.com/dissertations-theses/iot-based-air-quality-monitoring-system-with/docview/2647209830/se-2

13. Abreu, A., Lopes, S. I., Manso, V., & Curado, A. (2020). Low-cost LoRa-based IoT edge device for indoor air quality management in schools. In *2020 International summit smart city 360° (SmartCity 360°'2020)* (pp. 246–258). https://doi.org/10.1007/978-3-030-76063-2_18
14. Ajayi, O. O., Bagula, A. B., Maluleke, H. C., Gaffoor, Z., Jovanovic, N., & Pietersen, K. C. (2022). WaterNet: A network for monitoring and assessing water quality for drinking and irrigation purposes. *IEEE Access, 10*, 48318–48337. https://doi.org/10.1109/ACCESS.2022.3172274
15. Brindha, S., Abirami, P., Srikanth, V. P., Raj, A. A., & Raja, K. K. (2019). Efficient water management using LoRa in advance IoT. *International Journal of Research in Engineering, Science and Management, 2*(3), 834–837.
16. Zhao, G., Lin, K., & Hao, T. (2023). A feasibility study of LoRaWAN-based wireless underground sensor networks for underground monitoring. *Computer Networks, 232*, 109851. https://doi.org/10.1016/j.comnet.2023.109851
17. Adi, P. D. P., & Wahyu, Y. (2023). The error rate analyze and parameter measurement on LoRa communication for health monitoring. *Microprocessors and Microsystems, 98*, 104820. https://doi.org/10.1016/j.micpro.2023.104820
18. Santana, J. R., Stores, P., Pérez, J., Sánchez, L., Lanza, J., & Muñoz, L. (2023). Assessing LoRaWAN radio propagation for smart parking service: An experimental study. *Computer Networks, 235*, 109962. https://doi.org/10.1016/j.comnet.2023.109962
19. Yasmin, R., Petäjäjärvi, J., Mikhaylov, K., & Pouttu, A. (2018). Large and dense LoRaWAN deployment to monitor real estate conditions and utilization rate. In *2018 IEEE 29th annual international symposium on personal indoor and mobile radio communications (PIMRC'2018)* (pp. 1–6). https://doi.org/10.1109/PIMRC.2018.8580985
20. Parri, L., Parrino, S., Peruzzi, G., & Pozzebon, A. (2021). Offshore LoRaWAN networking: Transmission performances analysis under different environmental conditions. *IEEE Transactions on Instrumentation and Measurement*, *70*, 1–10, Art no. 9507710. https://doi.org/10.1109/TIM.2020.3031193
21. To, T. H., & Duda, A. (2018). Simulation of LoRa in NS-3: Improving LoRa performance with CSMA. In *2018 IEEE international conference on communications* (ICC'2018) (pp. 1–7). https://doi.org/10.1109/ICC.2018.8422800
22. Ta, D. T., Khawam, K., Lahoud, S., Adjih, C., & Martin, S. (2019). LoRa-MAB: A flexible simulator for decentralized learning resource allocation in IoT networks. In *2022 12th IFIP conference on wireless and mobile networking* (WMNC'2019) (pp. 55–62). https://doi.org/10.23919/WMNC.2019.8881393
23. Citoni, B., Ansari, S., Abbasi, Q. H., Imran, M. A., & Hussain, S. (2022). Comparative analysis of an urban LoRaWAN deployment: Real world versus simulation. *IEEE Sensors Journal, 22*(17), 17216–17223. https://doi.org/10.1109/JSEN.2022.3193504
24. Wu, W., Wang, H., & Cheng, Z. (2023). ReLoRaWAN: Reliable data delivery in LoRaWAN networks with multiple gateways. *Ad Hoc Networks, 147*, 103203. https://doi.org/10.1016/j.adhoc.2023.103203
25. Adeunis Field Test Device. https://www.adeunis.com/en/produit/ftd-network-tester/
26. Jeftenić, N., Simić, M., & Stamenković, Z. (2020). Impact of environmental parameters on SNR and RSS in LoRaWAN. In *2020 International conference on electrical, communication, and computer engineering (ICECCE'2020)*. https://doi.org/10.1109/ICECCE49384.2020.9179250
27. Montagny S. (2023). *LoRa—LoRaWAN and Internet of Things.* https://www.univ-smb.fr/lorawan/en/free-book/
28. Sinha, R. S., Wei, Y., & Hwang, S. H. (2017). A survey on LPWA technology: LoRa and NB-IoT. *ICT Express, 3*(1), 14–21. https://doi.org/10.1016/j.icte.2017.03.004
29. Gu, F., Niu, J., Jiang, L., Liu, X., & Atiquzzaman, M. (2020). Survey of the low power wide area network technologies. *Journal of Network and Computer Applications, 149*, 102459. https://doi.org/10.1016/j.jnca.2019.102459
30. de Almeida, I. B. F., Chafii, M., Nimr, A., & Fettweis, G. (2021). Alternative chirp spread spectrum techniques for LPWANs. *IEEE Transactions on Green Communications and Networking, 5*(4), 1846–1855. https://doi.org/10.1109/TGCN.2021.3085477
31. Adi, P. D. P., Wahyu, Y., & Kitagawa, A. (2022). Analyzes of chirps spread spectrum of ES920LR LoRa 920 MHz. In *2022 11th electrical power, electronics, communications, controls and informatics seminar* (EECCIS'2022) (pp. 139–144). https://doi.org/10.1109/EECCIS54468.2022.9902922
32. Pasolini, G. (2022). On the LoRa chirp spread spectrum modulation: Signal properties and their impact on transmitter and receiver architectures. *IEEE Transactions on Wireless Communications, 21*(1), 357–369. https://doi.org/10.1109/TWC.2021.3095667
33. Lopez Chalacan, V. H. L. (2020). Performance evaluation of long range (LoRa) wireless RF technology for the Internet of Things (IoT) using Dragino LoRa at 915 MHz. M.Sc. thesis, University

of North Florida. https://www.proquest.com/dissertations-theses/performance-evaluation-long-range-lora-wireless/docview/2519440999/se-2
34. Spreading Factors. (2022). https://www.thethingsnetwork.org/docs/lorawan/spreading-factors/
35. Attia, T., Heusse, M., Tourancheau, B., & Duda, A. (2019). Experimental characterization of LoRaWAN link quality. In *2019 IEEE global conference on communications* (GLOBECOM'2019). https://doi.org/10.1109/GLOBECOM38437.2019.9013371
36. LoRa Alliance. (2023). https://lora-alliance.org/
37. LoRaWAN Architecture. (2023). https://www.thethingsnetwork.org/docs/lorawan/spreading-factors/
38. Device Classes (2023). https://www.thethingsnetwork.org/docs/lorawan/classes/
39. Pereira, F., Lopes, S. I., Carvalho, N. B., & Curado, A. (2020). RnProbe: A LoRa-enabled IoT edge device for integrated radon risk management. *IEEE Access, 8*, 203488–203502. https://doi.org/10.1109/ACCESS.2020.3036980
40. Peruzzi, G., Pozzebon, A., & Van Der Meer, M. (2023). Fight fire with fire: Detecting forest fires with embedded machine learning models dealing with audio and images on low power IoT devices. *Sensors, 23*(2), 783. https://doi.org/10.3390/s23020783
41. Boccadoro, P., Montaruli, B., & Grieco, L. A. (2019). Quakesense, a LoRacompliant earthquake monitoring open system. In *2019 IEEE/ACM 23rd international symposium on distributed simulation and real time applications (DS-RT'2019)*. https://doi.org/10.1109/DS-RT47707.2019.8958675
42. Panicker, J. G., Azman, M., & Kashyap, R. (2019). A LoRa wireless mesh network for wide-area animal tracking. In *2019 IEEE international conference on electrical, computer and communication technologies (ICECCT'2019)*. https://doi.org/10.1109/ICECCT.2019.8868958
43. Bathre, M., & Das, P. K. (2022). Water supply monitoring system with self-powered LoRa based wireless sensor system powered by solar and hydroelectric energy harvester. *Computer Standards and Interfaces, 82*, 103630. https://doi.org/10.1016/j.csi.2022.103630
44. Alghamdi, A. M., Khairullah, E. F., & Al Mojamed, M. M. (2022). LoRaWAN performance analysis for a water monitoring and leakage detection system in a housing complex. *Sensors, 22*(19), 7188. https://doi.org/10.3390/s22197188
45. LoRa Physical Layer Packet Format. (2023). https://www.thethingsnetwork.org/docs/lorawan/lora-phy-format/

Ataberk Aksoy graduated from Bursa Uludağ University, Department of Electrical and Electronics Engineering, Bursa, Türkiye in 2021. He is currently going toward his M.Sc. degree in Electronics Engineering at Bursa Uludağ University. He is studying wireless communication in graduate school.

Ömer Yıldız received his B.Sc. degree in electronics and communication engineering from Yıldız Technical University, Istanbul, Türkiye in 2008 and his M.Sc. degree in electronics engineering from Uludağ University, Bursa, Türkiye in 2019. Currently, he is a Ph.D. candidate in Electrical and Electronics Engineering Department of Bursa Uludağ University. His research interests involve wireless networks, IoT, LPWAN and biomedical technologies.

Sait Eser Karlık received his B.Sc. degree in electronics and communication engineering from Istanbul Technical University, Istanbul, Türkiye in 1997 and his M.Sc. and Ph.D. degrees in electronics engineering from Uludağ University, Bursa, Türkiye in 1999 and 2006, respectively. Currently, he is working as an Associate Professor in Electrical and Electronics Engineering Department of Bursa Uludağ University. His research interests involve long-haul and access networks, nonlinear phenomena in optical fibers and LPWAN technologies.